The Family 1 β-Glucosidases from *Pyrococcus furiosus* and *Agrobacterium faecalis* Share a Common Catalytic Mechanism†

Michael W. Bauer‡ and Robert M. Kelly*

Department of Chemical Engineering, North Carolina State University, Raleigh, North Carolina 27695

Received June 23, 1998; Revised Manuscript Received September 29, 1998

ABSTRACT: Comparisons of catalytic mechanisms have not previously been performed for homologous enzymes from hyperthermophilic and mesophilic sources. Here, the β-glucosidase from the hyperthermophilic archaeon *Pyrococcus furiosus* was recombinantly produced in *Escherichia coli* and shown to have biophyscial and biochemical properties identical to those of the wild-type enzyme. Moreover, the recombinant enzyme was subjected to a detailed kinetic investigation at 95 °C to compare its catalytic mechanism to that determined at 37 °C for the β-glucosidase (abg) from the mesophilic bacterium, *Agrobacterium faecalis* [Kempton, J., and Withers, S. G. (1992) *Biochemistry 31*, 9961]. These enzymes have amino acid sequences that are 33% identical and have been classified as family 1 glycosyl hydrolases on the basis of amino acid sequence similarities. Both enzymes have similar broad specificities for both sugar and aglycone moieties and exhibit nearly identical pH dependences for their kinetic parameters with several different substrates. Brønsted plots were constructed for bgl at several temperatures using a series of aryl glucoside substrates. These plots were concave downward at all temperatures, indicating that bgl utilized a two-step mechanism similar to that of abg and that the rate-limiting step in this mechanism did not change with temperature for any given aryl glucoside. The Brønsted coefficient for bgl at 95 °C ($\beta_{1g} = -0.7$) was identical to that for abg at 37 °C and implies that these enzymes utilize nearly identical transition states, at least in regard to charge accumulation on the departing glycosidic oxygen. In addition, a high correlation coefficient ($\rho = 0.97$) for the linear free energy relationship between these two enzymes and similar inhibition constants for these two enzymes with several ground state and transition state analogue inhibitors further indicate that these enzymes stabilize similar transition states. The mechanistic similarities between these two enzymes are noteworthy in light of the large difference in their temperature optima. This suggests that, in the presumed evolution that occurred between the hyperthermophilic archaeal enzyme and the mesophilic bacterial enzyme, structural modifications must have been selected which maintained the integrity of the active site structure and, therefore, the specificity of transition state interactions, while adapting the overall protein structure to permit function at the appropriate temperature.

Hyperthermophilic microorganisms may be defined as those organisms that grow at ≥90 °C (*1*, *2*). On the basis of 16S rRNA sequence analysis, hyperthermophiles, especially the hyperthermophilic *Archaea*, have been placed close to the root of the phylogenetic tree, suggesting that they preceded mesophilic organisms (*3*−*5*). The discovery of hyperthermophilic organisms has led to the isolation of enzymes that, in some cases, function optimally at temperatures exceeding 100 °C (*6*, *7*). Comparisons between homologous enzymes from organisms with differing degrees of thermophilicity have subsequently been carried out to gain insight into the underlying bases for protein stability (*8*−*15*). Although these studies have provided information about the structural factors affecting thermostability, complementary comparisons of catalytic mechanisms between hyperthermophilic and mesophilic enzymes have not yet been carried out. The key question in this regard is whether homologous enzymes from hyperthermophilic and mesophilic organisms catalyze reactions by similar mechanisms, despite large differences in the temperature optima. The answer to this question takes into account the influence of temperature on the evolution of both the overall protein tertiary structure and the architecture of the active site as well as the mechanism by which substrates are bound and converted to products.

The hyperthermophilic archaeon *Pyrococcus furiosus* is an obligately anaerobic heterotroph isolated from a shallow marine hydrothermal vent (*16*). It grows optimally at 98−100 °C (*16*) and can utilize a number of carbohydrates, including starch, pullulan, and maltose (*17*), as well as cellobiose (*18*) and laminarin (*19*). To assimilate these compounds, *P. furiosus* must necessarily produce several glycosyl hydrolases, including two amylases (*20*−*22*), an amylopullulanase (*17*, *23*), an α-glucosidase (*24*), a β-glucosidase (*18*, *25*, *26*), a β-mannosidase (*26*), and a laminarinase (*19*). The exact mechanism of action has been elucidated neither for these enzymes from *P. furiosus* nor

† This work was supported in part by grants from the National Science Foundation (BES-963267) and the Department of Energy (DE-FG02-96ER20219). M.W.B. acknowledges the support of a Department of Education GAANN Fellowship.

* To whom inquiries should be addressed: Department of Chemical Engineering, North Carolina State University, Raleigh, NC 27695-7905. Telephone: (919) 515-4452. Fax: (919) 515-3465. E-mail: rmkelly@eos.ncsu.edu.

‡ Present address: Novartis Agribusiness Biotechnology Research, Inc., 3054 Cornwallis Rd., Research Triangle Park, NC 27709.

10.1021/bi9814944 CCC: $15.00
Published on Web 11/12/1998

for any glycosyl hydrolase from a thermophilic organism nor for any glycosyl hydrolase from an archaeon.

The complete purification of the *P. furiosus* β-glucosidase (bgl)[1] has been described (*18*). Characterization of the wild-type enzyme revealed that bgl was a homotetramer, with a subunit molecular mass of approximately 55 kDa. The substrate specificity of the wild-type enzyme was found to be relaxed, cleaving glycosidic linkages when glucose, galactose, xylose, and mannose were in the terminal, nonreducing position (*18*). The gene for the β-glucosidase has been cloned and expressed (*25*, *26*). On the basis of amino acid sequence similarities, bgl has been assigned to glycosyl hydrolase family 1 (*25*, *26*).

The catalytic mechanism of another family 1 enzyme, the β-glucosidase (abg) from the mesophilic bacterium *Agrobacterium faecalis*, has been extensively studied (*27*−*31*). The techniques used to characterize this enzyme include substrate specificity, pH dependences, kinetic isotope effects, linear free energy relationships (*27*), interactions with deoxy substrate analogues (*30*), affinity labeling (*29*), and site-directed mutagenesis (*28*, *31*). This paper describes a comparative study of the β-glucosidases from *P. furiosus* and *A. faecalis* focusing on their catalytic mechanisms. The results presented here provide insight into the mechanism of glycoside hydrolysis at elevated temperatures and allow direct comparison between the biochemical properties of abg and bgl, enzymes that have homologous amino acid sequences (56% similar and 33% identical) yet vastly different temperature optima. The similarities in the catalytic properties of these two enzymes suggest that the active site architecture has evolved far less than the overall protein structure.

MATERIALS AND METHODS

Materials. Phenyl, *o*-nitrophenyl, *p*-nitrophenyl, hydroquinone, and β-naphthyl glycosides, isopropyl β-D-thioglucopyranoside, 1-deoxynojirimycin, 1,6-anhydro-β-D-glucopyranose, gluconolactone, 2,3,4,6-tetra-*O*-acetyl α-D-glucopyranosyl bromide, and all buffer chemicals were obtained from Sigma Chemical Co., Aldrich Chemical Co., or Fluka. Synthesis of protected aryl glucosides was achieved from 2,3,4,6-tetra-*O*-acetyl α-D-glucopyranosyl bromide and the sodium salt of the corresponding phenol using the aqueous acetone method (*32*). Sensitive glucosides (phenol pK_a of <7) were deprotected using HCl in dry methanol (*33*), while other glucosides were deprotected using sodium methoxide in methanol (*34*). All products were obtained in crystalline form and characterized by melting point, ^{1}H NMR, and elemental analysis. These analyses were consistent with the expected structure and literature data, when available, in each case. For instance, melting points, determined for the deprotected substrates, were as follows: 4′-chlorophenyl β-D-glucopyranoside, 172−174 °C [lit. mp (*35*) 173−175 °C]; 4′-bromophenyl β-D-glucopyranoside, 169−172 °C [lit. mp (*27*) 175−176 °C]; 4′-*tert*-butylphenyl β-D-glucopyranoside, 144−146 °C [lit. mp (*35*) 145−146 °C]; 3′-nitrophenyl β-D-glucopyranoside, 167−169 °C [lit. mp (*35*) 166−168 °C]; 3′,5′-dichlorophenyl β-D-glucopyranoside, 215−218 °C [lit. mp (*27*) 215−217 °C]; 2′,4′,6′-trichlorophenyl β-D-glucopyranoside, 188−190 °C [lit. mp (*27*) 190−194 °C]; 3′,4′-dinitrophenyl β-D-glucopyranoside, 151−153 °C [lit. mp (*27*) 152−153 °C]; 4′-chloro-2′-nitrophenyl β-D-glucopyranoside, 160−162 °C [lit. mp (*27*) 159−160 °C]; *m*-cresyl β-D-glucopyranoside, 179−180 °C [lit. mp (*35*) 180 °C]; and 2′,4′-dichlorophenyl β-D-glucopyranoside, 172−174 °C.

Purification of the Native Protein. P. furiosus crude cell extract was prepared as described previously (*36*, *37*). The reported purification procedure for the β-glucosidase (*18*) was modified as follows; the crude cell extract was applied to a column (5 cm × 35 cm) of DEAE-Sepharose. After being washed with 7 L of 50 mM Tris-HCl (pH 8.0), the column was developed with a 5 L gradient from 0.0 to 0.5 M NaCl. Fractions were assayed for β-glucosidase activity at 95 °C using 1 mM PNPGlu. β-Glucosidase activity eluted between 380 and 420 mM NaCl. These fractions were pooled, concentrated, equilibrated with 25 mM potassium phosphate buffer (pH 7.0), and applied to a column (2.6 cm × 60 cm) of hydroxyapatite. After washing with 0.5 L of this buffer, the column was developed with a 1.5 L gradient from 25 to 500 mM potassium phosphate buffer (pH 7.0). β-Glucosidase activity eluted between 90 and 120 mM potassium phosphate. These fractions were pooled, concentrated, equilibrated with 50 mM sodium phosphate buffer containing 1.0 M ammonium sulfate, and applied to a column (1.6 cm × 20 cm) of Phenyl Sepharose. After washing with 30 mL of this buffer, the column was developed with a 180 mL gradient from 1.0 to 0.0 M ammonium sulfate. β-Glucosidase activity eluted between 200 and 150 mM ammonium sulfate. These fractions were pooled, concentrated, equilibrated with 50 mM sodium phosphate buffer (pH 7.0), and applied to a column (1.6 cm × 60 cm; V_e = 62 mL, V_t = 121 mL) of Superdex200 (Pharmacia). β-Glucosidase activity eluted as a symmetrical peak at 84 mL.

Production and Purification of Recombinant Protein. Recombinant *P. furiosus* β-glucosidase was purified from *Escherichia coli* as follows. Protein was expressed in *E. coli* BL21(DE3) cells (Novagen) from the T7 promoter of pET22 (Novagen). Cells were grown overnight in 10 mL of Luria broth with 100 mg/mL ampicillin (LB amp) at 37 °C. Five milliliters of a culture was used to inoculate 1 L of LB amp. Cultures were grown for 6 h and transferred to a 20 L fermentor (Bioengineering AG, model L1523) containing 15 L of LB amp. Cultures were grown at 37 °C until the OD_{600} reached 0.8, and IPTG was added to a final concentration of 1 mM. Cultures were harvested after 4 h and concentrated to 1 L by Pellicon-2 cross-flow ultrafiltration (Millipore) with a 10K polysulfone membrane. After centrifugation at 15000*g*, the cell pellet was resuspended in 2.5 v/w, 50 mM sodium phosphate buffer (pH 7.0). Cell extracts were prepared by lysing the cells by two passages through a French press (SLM Instruments) at 18 000 psi followed by centrifugation (20 min at 30000*g*). The soluble cell extract was incubated for 30 min at 80 °C, chilled to 4 °C, and centrifuged (30 min at 30000*g*). The heat-treated supernatant was loaded onto a column of DEAE-Sepharose (5 cm × 35 cm) which had been previously equilibrated with 50 mM sodium phosphate (pH 7.0). The column was developed with a 5 L linear gradient of 0 to 1 M sodium

[1] Abbreviations: bgl, *P. furiosus* β-glucosidase; abg, *A. faecalis* β-glucosidase; PNPGlu, *p*-nitrophenyl β-D-glucopyranoside; PNPMan, *p*-nitrophenyl β-D-mannopyranoside; PGlu, phenyl β-D-glucopyranoside; PNPAra, *p*-nitrophenyl α-L-arabinopyranoside; PNPXyl, *p*-nitrophenyl β-D-xylopyranoside.

chloride in the starting buffer. Fractions were assayed for β-glucosidase activity at 95 °C using 1 mM PNPGlu. Fractions containing β-glucosidase activity were pooled, equilibrated with 50 mM sodium phosphate buffer (pH 7.0), and loaded onto a column (1.6 cm × 60 cm) of Superdex200. β-Glucosidase activity eluted as a symmetrical peak at 84 mL. Fractions containing β-glucosidase activity were pooled and concentrated. The enzyme were judged to be homogeneous by SDS−PAGE. Protein concentrations were determined by a dye-binding method (*38*) using bovine serum albumin as the standard.

Kinetic Studies. All kinetic studies were performed by following changes in UV−vis absorbance using 1 cm path length, matched quartz cells in a Lambda 3B spectrophotometer (Perkin-Elmer), equipped with a circulating bath which contained 90% tetraethylene glycol/10% water capable of maintaining temperatures of up to 100 °C. The buffers employed for all kinetic experiments were 50 mM sodium acetate buffer (pH 3.6−5.6) and 50 mM sodium phosphate buffer (pH 5.4−8.2). Extinction coefficients for phenols were determined by measuring the absorbances of carefully prepared stock solutions of each compound in the same buffer at the appropriate temperature. The molar extinction coefficients (ϵ, M^{-1} cm^{-1}) determined for each phenol in 50 mM sodium phosphate buffer (pH 6.0) at 95 °C were as follows: 3′,4′-dinitrophenyl, 400 nm, 11 116; 2′,4′,6′-trichlorophenyl, 312 nm, 1930; 4′-chloro-2′-nitrophenyl, 425 nm, 2722; 4′-nitrophenyl, 400 nm, 4250; 2′-nitrophenyl, 400 nm, 955; 2′,4′-dichlorophenyl, 294 nm, 1260; 3′,5′-dichlorophenyl, 280 nm, 1180; 3′-nitrophenyl, 380 nm, 414; 4′-bromophenyl, 288 nm, 838; 4′-chlorophenyl, 278 nm, 808; β-naphthyl, 325 nm, 918; phenyl, 277 nm, 866; *m*-cresyl, 271 nm, 1090; hydroquinone, 290 nm, 2249; and 4′-*tert*-butylphenyl, 272 nm, 1150.

Rates of enzyme-catalyzed hydrolysis were determined by incubating the appropriate substrate in buffer in a 1 cm cuvette located in the thermostated block of the spectrophotometer until the temperature was stabilized at 95 °C (as determined using a separate cell containing a thermocouple). The enzyme was equilibrated to the assay temperature by submerging an Eppendorf tube containing the enzyme in a heat block containing silicon oil at the appropriate temperature. The reaction was initiated by the addition of enzyme to the substrate, and the reaction was monitored at the appropriate wavelength relative to a reference cuvette at the same temperature containing no enzyme. The rate of enzyme-catalyzed hydrolysis was determined at seven to ten different substrate concentrations ranging from approximately 0.15 times the value of the K_m ultimately determined to 7 times its value, when possible. Values of K_m and k_{cat}, as well as the errors associated with these values, were determined from these rates by means of nonlinear regression analysis (*39*). K_i values for inhibitors were determined by first estimating the approximate K_i value by varying the inhibitor concentration at a fixed concentration of substrate (1.0 mM PNPGlu) and plotting the data in a Dixon plot. A full K_i determination was then carried out at a series of seven to ten different substrate concentrations bracketing the K_m value with three to five inhibitor concentrations bracketing the approximate K_i value. All such data was fit using nonlinear regression analysis (*39*).

The pH dependence of the enzyme was investigated by determining k_{cat} and K_m values at a series of pH values between 3.6 and 8.2. The pH values were determined with an Accumet 15 pH meter (Fisher Scientific) at the appropriate temperature. The determination of pH dependences involved incubating the substrate in buffer at the desired pH and then adding thermally equilibrated enzyme to the substrate to start the reaction.

Calorimetry. Differential scanning calorimetry (DSC) analyses were carried out on a Nanoscan microcalorimeter (Calorimetry Sciences) operating in the temperature range of 20−125 °C. The cell was pressurized to 3 atm to allow operation above 100 °C. Purified native and recombinant β-glucosidase were dialyzed extensively against 10 mM sodium phosphate buffer (pH 6.0). The equilibrated native and recombinant proteins were scanned at 0.5 °C/min using concentrations of 2.7 and 3.0 μM, respectively. All enzyme scans were corrected using a buffer−buffer baseline. The partial specific volume of the proteins was determined from their amino acid compositions (see below) (*40*). The excess molar heat capacity was calculated after baseline subtraction (*41*); i.e., the baseline was obtained from the linear temperature dependence of the native state heat capacity.

N-Terminal Sequencing and Amino Acid Composition Analysis. Purified, homogeneous native, and recombinant β-glucosidase were denatured, separated by 12.5% SDS−polyacrylamide gel electrophoresis, and electroblotted onto a poly(vinylidene difluoride) membrane and Ponceau S stained (*42*). N-Terminal Edman degradation was performed using a liquid phase sequencer (Applied Biosystems, model 477A). Amino acid composition analysis was carried out on purified, homogeneous native, and recombinant enzymes. Proteins were hydrolyzed in a gas phase of HCl at 120 °C for 20 h and the resulting amino acids derivatized with phenyl isothiocyanate and quantified (*43*) using an Applied Biosystems derivatizer/PTC analyzer (420A/130A). Tryptophan was determined from the A_{280} after correction for tyrosine (*44*). The cysteine content was estimated by reaction with 5,5′-dithiobis(2-nitrobenzoic acid) (*45*).

HPLC Procedures for Product Characterization. Hydrolyses of PNPXyl and PNPAra were performed using both high and low substrate concentrations (20 and 0.5 mM for PNPXyl and 40 and 0.2 mM for PNPAra). Aliquots of reaction mixtures (100 μL) were transferred to a Centricon-3 microconcentrator (Amicon) and concentrated 10-fold by centrifugation (3000*g*). The filtrate was injected onto a Spectra-Physics 8800 HPLC system equipped with an Altima C18 column (Alltech), eluted with 40:60 water/methanol, and detected with a Waters 990 photodiode array detector (Millipore) operating between 190 and 500 nm. At high substrate concentrations, one new product appeared for each of these substrates which did not appear at low substrate concentrations. Fractions containing these new products were combined, lyophilized, and identified by mass spectrometry and ^{1}H NMR.

RESULTS

Substrate Specificities. Kinetic parameters for the recombinant and native versions of the *P. furiosus* β-glucosidase on a variety of substrates are presented in Table 1. For the recombinant enzyme, at the relatively low concentrations of

Table 1: Michaelis−Menten Parameters for the Hydrolysis of Aryl Glycosides by the *P. furiosus* β-Glucosidase[a] (bgl) and *A. faecalis* β-Glucosidase[b] (abg)

	K_m (mM)		k_{cat} (s^{-1})		k_{cat}/K_m (s^{-1} mM^{-1})	
phenyl glycoside substrate	bgl	abg	bgl	abg	bgl	abg
PNP β-D-glucopyranoside	0.20 (0.21)	0.078	480 (530)	169	2370 (2520)	2170
PNP β-D-galactopyranoside	4.7 (4.5)	5.0	1450 (920)	275	310 (210)	55
PNP β-D-mannopyranoside	2.2 (2.6)	0.02	56 (59)	0.12	26 (22)	6
PNP β-D-fucopyranoside	0.52 (0.34)	0.12	1180 (480)	139	2260 (1410)	1157
PNP β-D-xylopyranoside	(i)[c] 1.03	0.022	94	1.85	91.5	8.4
	(ii) 10	3.3	460	8.0	45.8	2.4
PNP α-L-arabinopyranoside	(i)[c] 0.21	0.33	33	32.6	160	98.9
	(ii) 53	nr[e]	630	nr	12	nr
PNP α-L-arabinofuranoside	23	nr	88	nr	3.6	nr
PNP β-D-6-deoxy-6-fluoro-glucopyranoside[d]	1.24	0.359	750	49.5	600	138
ONP β-D-xylopyranoside	(i)[c] 0.43	0.025	43	1.04	100	42
	(ii) 4.4	2.4	120	2.36	26	1.0
ONP β-D-galactopyranoside	2.96	9.3	2510	267	850	28.8

[a] Kinetic parameters are for the recombinant and native (in parentheses) versions of bgl. [b] The kinetic parameters for abg were taken from Kempton and Withers (*27*). [c] Parameters are for the (i) hydrolysis and (ii) transglycosylation reactions. [d] Data for abg were taken from Namchuk and Withers (*30*). [e] nr indicates that this kinetic parameter was not reported.

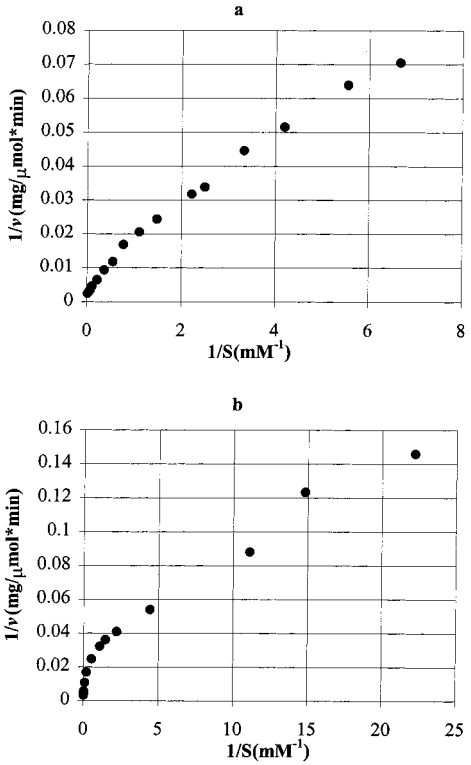

FIGURE 1: Lineweaver−Burk plot for the hydrolysis of (a) *p*-nitrophenyl xylopyranoside and (b) *p*-nitrophenyl arabinopyranoside by bgl at 95 °C.

substrate studied in most cases (up to approximately 10 times the K_m value), there was no evidence of transglycosylation through the transfer to another molecule of substrate. However, the Lineweaver−Burk plots for two substrates, *p*-nitrophenyl β-D-xylopyranoside and *p*-nitrophenyl α-L-arabinopyranoside, were biphasic (Figure 1a,b), revealing a rate enhancement over that expected at higher substrate concentrations. This has been observed to occur with the β-glucosidase from *A. faecalis* with PNPXyl and has been attributed to a transglycosylation reaction (*27*). For bgl, mass spectrometry and ^{1}H NMR of the reaction products confirmed that transglycosylation was occurring. Values of k_{cat} and K_m for both the hydrolytic reaction and the transglycosylation reaction were estimated by drawing a straight line through the two regions of the Lineweaver−Burk plot. Such an approach was used to estimate these two parameters for abg (*27*).

Table 2: Inhibition Constants for bgl and abg[a]

	K_i (mM)	
inhibitor	bgl	abg
glucose	40	6.4
isopropyl β-D-thioglucoside	8.0	4.0
gluconolactone	0.080	0.0014
1-deoxynojirimycin	0.05	0.05
1,6-anhydro-β-glucopyranose	190	190
tris(hydroxymethyl)aminomethane	1.3	0.5

[a] The inhibition constants for abg were taken from Kempton and Withers (*27*) and Day and Withers (*46*).

Inhibitor Studies. Inhibition constants (K_i values) for a series of competitive inhibitors are shown in Table 2. Several of the inhibitors (i.e., glucose and IPTGlu) mimic the ground state, while others (i.e., 1-deoxynojirimycin and gluconolactone) resemble the proposed transition state of the catalyzed reaction.

Substrate Reactivities. The k_{cat} and K_m values determined at 95 °C for a series of aryl glucoside substrates containing phenols with differing leaving abilities (as measured by the pK_a of the phenol) are presented in Table 3. The Brønsted relationships between reaction rate and leaving group ability for these substrates are presented in Figure 2a−c. From the Brønsted plot for bgl at 95 °C, the dependence of k_{cat} on leaving group ability was linear with a slope (Brønsted coefficient, β_{lg}) of −0.7 for substrates with poor leaving groups (pK_a > 9). This agrees with the Hammett coefficient of 1.5 determined for para-substituted phenyl glycosides (Figure 2d). The Brønsted plots for bgl at 70 and 45 °C had the same concave downward shape as the plot at 95 °C, indicating that all substrates had the same rate-limiting step in this temperature range. A linear free energy relationship between bgl and abg was obtained from kinetic data for PNP glycosides and aryl glucosides (Figure 3). A high correlation coefficient (ρ = 0.97) was observed, indicating similar interactions within the active sites for these two enzymes (*51*).

Table 3: Michaelis−Menten Parameters for the Hydrolysis of Aryl Glucosides by bgl and abg[a]

phenol substituent	pK_a[b]	k_{cat} (s^{-1})		K_m (mM)		k_{cat}/K_m (s^{-1} mM^{-1})	
		bgl	abg	bgl	abg	bgl	abg
3,4-dinitro	5.36	510	185	0.17	0.033	3030	5600
2,4,6-trichloro	6.39	820	240	0.059	0.009	14000	26000
4-chloro-2-nitro	6.45	600	144	0.135	0.013	4400	11000
4-nitro	7.18	480	169	0.203	0.078	2370	2200
2-nitro	7.22	950	111	0.281	0.033	3300	3400
2,4-dichloro	7.85	490	nr[c]	0.19	nr	2600	nr
3,5-dichloro	8.19	370	159	0.12	0.13	3090	1200
3-nitro	8.39	530	108	0.234	0.19	2280	570
4-bromo	9.34	390	28.8	0.70	0.56	550	52
4-chloro	9.38	370	29.6	0.82	0.64	450	46
2-naphthyl	9.51	300	25.3	0.576	0.16	521	160
H (phenol only)	9.99	270	5.4	2.71	2.12	100	3
3-cresol	10.08	120	nr	0.66	nr	180	nr
hydroquinone	10.35	59	nr	5.93	nr	10	nr
4-*tert*-butyl	10.37	74	5.13	0.26	0.069	290	74

[a] Data for abg were taken from Kempton and Withers (*27*). [b] Data for phenol pK_a were taken from reported values at 25 °C (*47*−*50*).[c] nr indicates that these values were not reported.

pH Dependences. Values of k_{cat} and K_m at a series of pH values between 3.6 and 8.2 were determined with two different substrates, PNPGlu and PGlu (Figure 4a,b). In this pH range, values of k_{cat} for each substrate depend on two ionizations as follows: PNPGlu, pK_1 = 5.0 and pK_2 = 7.4; and PGlu, pK_1 = 4.4 and pK_2 = 7.2. Values of k_{cat}/K_m likewise depend on two ionizations as follows: PNPGlu, pK_1 = 4.3 and pK_2 = 7.2; and PGlu, pK_1 = 4.0 and pK_2 = 7.0.

Thermal Activity and Stability. Arrhenius plots based on k_{cat} were linear for the *P. furiosus* β-glucosidase with seven different aryl glucosides (data not shown), supporting the observation based on the Brønsted plots that the rate-limiting step was unchanged by temperature for any given substrate. Activation energies determined for these substrates are presented in Table 4. In addition, differential scanning calorimetry showed that both the native and recombinant proteins maintained a constant conformation below 100 °C and that both denatured irreversibly at 108 °C (Figure 5).

DISCUSSION

Comparison of the Recombinant Enzyme with the Wild Type. Direct comparison of biochemical and biophysical properties of the recombinant β-glucosidase with those previously reported for the wild-type enzyme isolated from *P. furiosus* (*18*, *26*) was hindered by differences in the methods used to characterize these enzymes. Therefore, both recombinant and wild-type enzymes were purified and characterized using identical procedures. The two types of enzyme had identical electrophoretic mobilities and retention times as determined by gel filtration chromatography. Moreover, they had identical N-terminal and amino acid compositions. In addition, the native and recombinant enzymes had identical relative substrate specificities, similar kinetic parameters, and identical denaturation temperatures of 108 °C as determined by microcalorimetry. These results indicate that the recombinant enzyme produced in *E. coli* has biophysical and biochemical properties comparable to those of the wild-type enzyme from *P. furiosus*.

Substrate Specificities. Both versions of the *P. furiosus* β-glucosidase have broad specificities as shown in Table 1. This broad specificity is common among glycosyl hydrolases from family 1, including the β-glucosidases from the mesophilic bacterium *A. faecalis* (abg) (*27*) and the thermophiles *Thermotoga maritima* (*52*) and *Sulfolobus solfataricus* (*53*, *54*). Both abg and bgl have the highest catalytic efficiency for pyranose substrates in which all the ring hydroxyls are equitorial (i.e., when glucose is the substrate). Moreover, the catalytic efficiencies of these two enzymes are nearly identical at temperatures representative of their native environments. However, if the equatorial hydroxyls at C4 or C2 of glucose are changed to the axial orientation, as in galactose or mannose, then the catalytic efficiencies of both bgl and abg decrease by 1 and 2 orders of magnitude, respectively. This indicates that the interactions that occur between the substrate binding pockets of bgl and abg and the specific orientations of the hydroxyls on the pyranose ring at the transition state have similar relative magnitudes. Although crystal structures are not available for bgl or abg, the structure has been determined for the family 1 myrosinase from *Sinapsis alba*, covalently attached to the mechanism-based inhibitor 2-deoxy-2-fluoroglucose. On the basis of this structure, five residues, Q39, H141, Y330, W457, and E464 (*S. alba* numbering), form hydrogen bonds with the bound inhibitor. The C3 hydroxyl forms H-bonds with Q39 and H141, the C4 hydroxyl H-bonds with Q39, W457, and E464, the C6 hydroxyl H-bonds with E464, and the ring oxygen H-bonds with Y330. All of these residues are present in bgl and abg and likely participate in similar H-bonding interactions.

The interaction between bgl and the substituent on C5 is noteworthy for two reasons. First, bgl not only hydrolyzes substrates with a C5 hydroxymethyl substituent, such as glucopyranose and galactopyranose, but also hydrolyzes substrates which lack these groups, such as xylopyranose (glucopyranose without a C5 hydroxymethyl substituent) and arabinopyranose (galactopyranose without a C5 hydroxymethyl) with 30- and 2-fold decreases in efficiency, respectively. Thus, interactions at the 6-position are moderately important for stabilizing the transition state in the first irreversible step (i.e., glycosylation). An estimate of the strength and polarity of this interaction can be obtained by comparisons among the kinetic parameters of glucose, its 6-deoxyfluoro analogue, and xylose. Replacement of the C6 hydroxyl with a fluorine should only allow hydrogen bonds in which the fluorine is an acceptor (*30*). The greater relative catalytic efficiency for 6-deoxyfluoroglucose than for xylose indicates that some of the binding energy lost by removal of the C5 hydroxymethyl is regained upon addition of the fluoromethyl substituent, and therefore, the enzyme likely donates a hydrogen bond at this location. Moreover, the magnitude of this bond may be estimate from (*30*, *55*)

$$\Delta\Delta G^{\circ\ddagger} = RT \ln[(k_{cat}/K_m)_{par}/(k_{cat}/K_m)_{sub}]$$

where $\Delta\Delta G^{\circ\ddagger}$ is the activation free energy change upon substitution and $(k_{cat}/K_m)_{par}$ and $(k_{cat}/K_m)_{sub}$ are the catalytic efficiencies for the parent (PNPGlu) and substituted glucoside (6-deoxyfluoro or xylose), respectively. Hence, for bgl, approximately 10 kJ mol^{-1} of binding energy is lost upon removal of the C5 hydroxymethyl (vs 16.3 kJ mol^{-1} for abg) and 5.8 kJ mol^{-1} (vs 8.6 kJ mol^{-1} for abg) is regained upon addition of the fluoromethyl substituent, although this is still

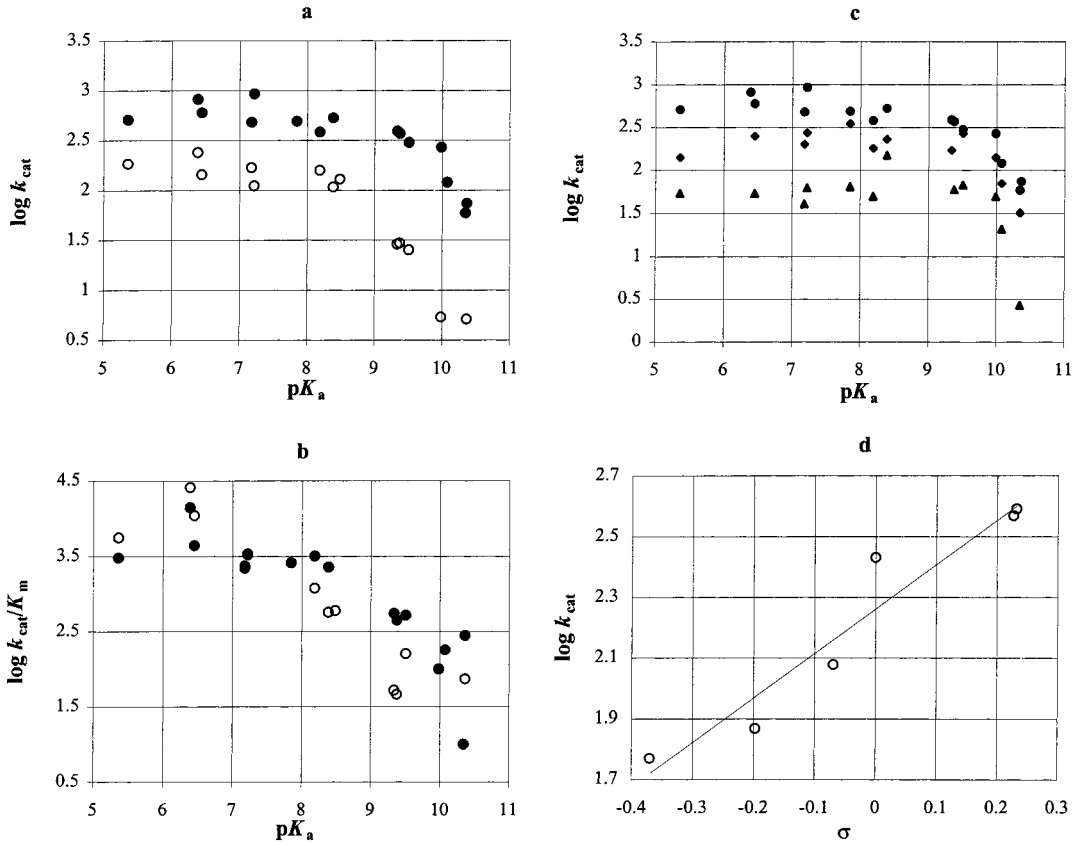

FIGURE 2: Brønsted and Hammett plots relating turnover numbers and catalytic efficiencies with the leaving group abilities of the substituted phenols. (a) Plot of log k_{cat} vs pK_a of the aglycone for bgl (●) and abg (○)-catalyzed hydrolysis of aryl glucosides at 95 and 37 °C, respectively. (b) Plot of log k_{cat}/K_m vs pK_a of the aglycone for bgl (●) and abg (○)-catalyzed hydrolysis of aryl glucosides at 95 and 37 °C, respectively. (c) Plot of log k_{cat} vs pK_a of the aglycon phenol for bgl at 95 (●), 70 (◆), and 45 °C (▲). (d) Plot of log k_{cat} vs Hammett coefficient for the hydrolysis of para-substituted phenyl glycosides by bgl at 95 °C. Data for abg were reported previously (*27*).

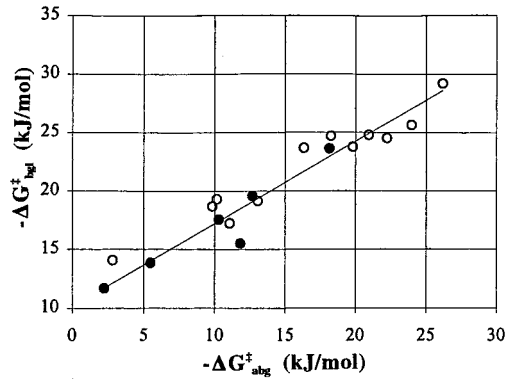

FIGURE 3: Linear free energy relationship between abg and bgl for a series of PNP glycosides (●) and aryl glucosides (○) (data are presented in Tables 1 and 3, respectively). The free energy of activation, $\Delta G^{\ddagger}$, was calculated from $\Delta G^{\ddagger} = -RT \ln k_{cat}/K_m$, where $T = 310$ K for abg and $T = 368$ K for bgl. Data for abg were reported previously (*27*, *46*).

4.2 kJ mol^{-1} less energy than for the parent substate. A similar polarity, although with a slightly greater magnitude (7.7 kJ mol^{-1}), was seen for the interaction at the 6-position for the β-glucosidase from *A. faecalis* (*30*).

The interaction between bgl and the substituent on C5 is also important for another reason. The *P. furiosus* β-glucosidase was observed to catalyze transglycosylation with two substrates, PNPXyl and PNPAra. Transglycosylation was also observed for abg with xylopyranoside substrates (*27*). These two compounds have a common structural characteristic that the other substrates in Table 1 lack; namely, both of these compounds lack a C5 substituent. Thus, the absence of a C5 substituent, and possibly its associated steric interactions, may be an important determinant for transglycosylation by bgl and abg.

Proposed Mechanism of Action. The family 1 β-glucosidase (abg) from *A. faecalis* was shown to follow the reaction pathway shown in Scheme 1(*27*, *30*). This is a double-displacement involving initial binding (rate constant of k_1) and unbinding (rate constant of k_{-1}) of the substrate to the enzyme to form a Michaelis complex (ES). This is followed by general acid-catalyzed attack (rate constant of k_2) by an enzymic nucleophile on the anomeric center to form a covalent glycosyl−enzyme intermediate (E−S). The glycosyl−enzyme intermediate is hydrolyzed (rate constant of k_3) by general base-catalyzed reaction of water with the anomeric carbon. The transition states leading to and from the covalent enzyme−substrate intermediate are believed to resemble oxocarbonium ions (*27*, *56*, *57*).

Evidence for a Two-Step Mechanism: Structure−Reactivity Studies. On the basis of structure−reactivity studies, the family 1 β-glucosidase (bgl) from *P. furiosus* appears to utilize a mechanism identical to that of abg. The biphasic nature of the Brønsted plot supports the notion of a two-step mechanism, the first step being glycosylation of the enzyme to form a covalent glycosyl−enzyme intermediate and the last step being hydrolysis, or deglycosylation, of this species. Substrates with good leaving groups (i.e., low pK_a) should have similar turnover numbers determined by the rate-limiting, leaving group-independent deglycosylation step. As

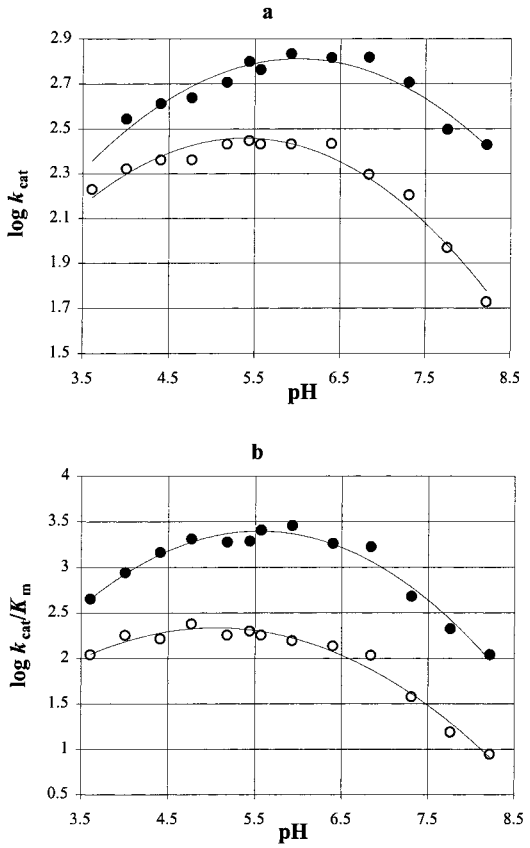

FIGURE 4: pH dependence of the hydrolysis of aryl glucosides by bgl. Kinetic parameters are indicated for (a) k_{cat} and (b) k_{cat}/K_m with PNPGlu (●) and PGlu (○).

Table 4: Activation Energies for bgl with Various Aryl Glucosides

phenol substituent	pK_a[a]	E_A (kJ/mol)[b]
4-nitro	7.18	49.3
2-nitro	7.22	45.8
2,4-dichloro	7.85	42.9
3,5-dichloro	8.19	40.3
2-naphthyl	9.51	40.8
H (phenol only)	9.99	31.3
3-cresol	10.08	36.3

[a] Data for phenol pK_a at 25 °C (*47*−*50*). [b] Values determined from Arrhenius plots for the range of 45−95 °C.

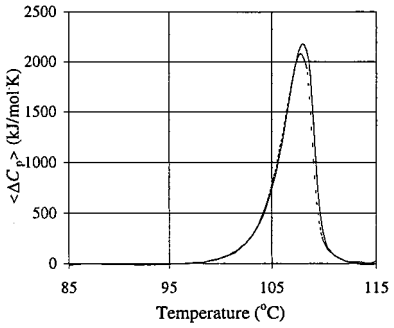

FIGURE 5: Thermal denaturation curves determined by differential scanning calorimetry for the recombinant (solid line) and native (dashed line) forms of the β-glucosidase from *P. furiosus*.

shown in Figure 2a,c, k_{cat} values are independent of the reactivity of the phenol group (as measured by the pK_a of the phenol, for pK_as of <9).

Conversely, for substrates with poor leaving groups (i.e., high pK_a), glycosylation should become rate-limiting and

Scheme 1

$$E + S \underset{k_{-1}}{\overset{k_1}{\rightleftharpoons}} ES \xrightarrow{k_2} E\text{-}S \xrightarrow{k_3} EP$$

$$K_m = \frac{k_{-1} + k_2}{k_1}\frac{k_3}{k_2 + k_3} \qquad k_{cat} = \frac{k_2 k_3}{k_2 + k_3} \qquad k_{cat}/K_m = \frac{k_1 k_2}{k_{-1} + k_2}$$

turnover numbers for these substrates should be proportional to the reactivity of the phenol group. As shown in Figure 2a, k_{cat} values depend on the reactivity of the phenol groups for phenol pK_as of >9. The slope of the line in this portion of the Brønsted plot for the first-order rate constant (k_{cat}) has a coefficient of −0.7. This is further supported by a Hammett coefficient ($\rho = 1.5$) for these substrates (Figure 2d) which is 70% of the value for that for the aqueous dissociation of phenols ($\rho = 2.23$) (*58*). This substantiates the supposition that formation of the glycosyl−enzyme intermediate is rate-determining for substrates with poor leaving groups and indicates that there is a large degree of bond cleavage at the transition state for bgl (*59*). Moreover, this value is identical to the reaction constant determined for abg ($\beta_{1g} = -0.7$) (*27*), indicating that the transition states for these two enzymes are nearly identical, at least in regard to the negative charge accumulation on the departing glycosidic oxygen. The high correlation coefficient for the linear free energy relationships further indicates that the two enzymes stabilize transition states with very similar structures (*51*). Furthermore, this Brønsted coefficient indicates that there is a large degree of bond cleavage at the transition state for both of these enzymes (*59*), although the extent of bond cleavage cannot be determined due to the unknown amount of proton donation.

The similarity of the Brønsted plots for bgl at 45, 70, and 95 °C is significant because it indicates that the rate-limiting step in the catalytic mechanism does not change with temperature for bgl. In other words, within the temperature range examined, the catalytic mechanism for the *P. furiosus* β-glucosidase is the same regardless of the temperature. In fact, this suggests that bgl uses the same catalytic mechanism as abg not only at high temperatures but also at temperatures where abg is also active. However, in the regime where both enzymes are active (i.e., below 50 °C), the *P. furiosus* enzyme is a less efficient enzyme than the *A. faecalis* enzyme.

The Brønsted plot for the second-order rate constant (k_{cat}/K_m) (Figure 2b) is also concave downward. This was also observed for abg (*27*). The biphasic nature cannot be related to a change from rate-limiting glycosylation to rate-limiting deglycosylation at higher reactivities because the second-order rate constant (k_{cat}/K_m) is independent of deglycosylation. Instead, it may reflect a change in the rate of enzyme−substrate association (k_1) relative to the rate of glycosylation as the phenol reactivity increases. Thus, the association of the free enzyme and substrate in solution may become rate-limiting at higher reactivities.

Inhibitor Studies. The K_i values presented in Table 2 indicate that the *P. furiosus* and *A. faecalis* enzymes have similar relative affinities for a variety of inhibitors and that they likely stabilize similar oxocarbonium ion transition states. Both enzymes have low affinities (e.g., K_i values on the order of 10 mM) for inhibitors with a chair conformation,

such as glucose and isopropyl β-D-thioglucopyranoside, and even lower affinities for inhibitors with a boat conformation, such as 1,6-anhydro-β-D-glucopyranose. However, both enzymes have much higher affinities for inhibitors which are similar to the proposed oxocarbonium ion transition state. For instance, gluconolactone assumes a half-chair conformation and may possess a positive charge on the ring oxygen (*57*) and, correspondingly, is one the most potent inhibitors of bgl. The *P. furiosus* β-glucosidase also has a strong affinity for the inhibitor 1-deoxynojirimycin. Despite the chair conformation of this compound, inhibition likely results from strong electrostatic interactions with the positive charge character at the ring nitrogen in the protonated form of this inhibitor (*60*).

pH Dependences. The *P. furiosus* enzyme has pH dependences for several different substrates which are essentially the same as those of the family 1 β-glucosidase from *A. faecalis* (*27*). This indicates that the strength and orientation of the specific hydrogen bonds that occur between the catalytic amino acids and the other active site residues in these two enzymes may also be very similar. This is further supported by comparison of the ionization constants for these enzymes in enzyme−substrate complexes (k_{cat} vs pH plots) and for the free enzymes in solution (k_{cat}/K_m vs pH plots). For bgl, catalysis depends on a protonated group with a pK_a of 7.0−7.4, whereas for abg, catalysis depends on a similar protonated group with a pK_a of 7.6−8.1 (*27*). The lower pK_a of the *P. furiosus* enzyme may indicate that there are slightly different interactions of the catalytic acid and/or base residues within the active sites of the *P. furiosus* and *A. faecalis* enzymes. Although, this is difficult to determine in the absence of crystal structures and may, instead, reflect changes in ionization for groups not in the active site which, nonetheless, affect catalytic activity.

Conclusions. Enzymes from hyperthermophilic organisms have been examined in relation to homologous enzymes from less thermophilic counterparts to obtain information concerning the intrinsic bases for thermostabilization. Although no universal strategies for affecting protein thermostability have been apparent (*6*, *12*), structural studies with the family 1 β-glucosidase from *S. solfataricus* (*14*) have indicated that the *S. solfataricus* protein has significantly more ion pairs on the surface of the protein and more buried solvent molecules in the interior of the protein than comparable proteins from mesophilic organisms. In the structure of the *S. solfataricus* β-glucosidase, these interactions occur in networks which are not found in the structure of the mesophilic family 1 β-glucosidase from *Trifolium repens* (*14*, *61*). These interactions may account for the greater thermostability of the hyperthermophilic protein by providing a degree of resiliency that dampens the molecular vibrations associated with the increased kinetic energy within the protein structure at elevated temperatures (*14*). The *P. furiosus* and *S. solfataricus* enzymes have amino acid sequences that are greater than 50% identical, and both are stable at temperatures up to 100 °C. All of the residues indicated to interact with buried solvent molecules in the *S. solfataricus* enzyme (*14*) are also found in the *P. furiosus* enzyme. In the absence of structural information for the *P. furiosus* enzyme, it remains to be seen how the extent of ion pairing observed in the *S. solfataricus* structure relates to the situation for the more thermostable glucosidase. Clearly, similar interactions would seem to also stabilize the structure of the *P. furiosus* β-glucosidase against thermal denaturation relative to the *A. faecalis* structure.

Several results indicate that the family 1 β-glucosidases from *P. furiosus* and *A. faecalis* have similar active sites or, at least, stabilize very similar transition states, including identical Brønsted coefficients (−0.7), a high correlation coefficient ($\rho = 0.97$) for the linear free energy relationship between the two enzymes, and similar interactions (both magnitude and polarity) with deoxy substrate analogues. For bgl to accommodate a similar transition state as abg at significantly higher temperatures (i.e., 95 vs 37 °C), the active site structure of the *P. furiosus* enzyme must adjust to the increased vibrational, rotational, and translational energy of the substrate. Structural resiliency not only may raise "the kinetic energy barrier to unfolding" for hyperthermophilic proteins (*14*) but also may allow these enzymes to absorb the greater kinetic energy or greater amplitude of molecular motions associated with substrates within their active sites at elevated temperatures.

Thus, if it is assumed that life on earth originated in hydrothermal environments (*2*, *5*), as organisms have adapted to lower temperatures, numerous subtle changes over the entire protein structure must necessarily have occurred to accommodate biocatalytic activity. From the results presented here for the family 1 β-glucosidases from *P. furiosus* and *A. faecalis*, it would seem that such changes did not compromise the catalytic activity of these enzymes. This is reasonable if viewed in the context of the overall physiological function of these enzymes. The cascade of reactions occurring within a cell must be orchestrated in such a way that metabolism can proceed. Only those changes in protein structure that were consistent with the thermal environment, without affecting catalytic properties, would have persisted for key metabolic enzymes. In this regard, evolution within a given set of homologous enzymes may be viewed as adapting the overall structural flexibility to accommodate the thermostability (a global structural parameter) and the active site architecture (a local structural parameter) within the context of the thermal environment.

REFERENCES

1. Baross, J. A., and Holden, J. F. (1996) *Adv. Protein Chem. 48*, 1−34.
2. Stetter, K. O. (1996) *FEMS Microbiol. Rev. 18*, 149−158.
3. Woese, C. R., and Fox, G. E. (1977) *Proc. Natl. Acad. Sci. U.S.A. 74*, 5088−5090.
4. Woese, C. R. (1987) *Microbiol. Rev. 51*, 221.
5. Woese, C. R., Kandler, O., and Wheelis, M. L. (1990) *Proc. Natl. Acad. Sci. U.S.A. 87*, 4576−4579.
6. Adams, M. W. W., Perler, F. B., and Kelly, R. M. (1995) *Bio/Technology 13*, 662−668.
7. Bauer, M. W., Halio, S. B., and Kelly, R. M. (1996) *Adv. Protein Chem. 48*, 271−310.
8. Day, M. W., Hsu, B. T., Joshua-Tor, L., Park, J.-B., Zhou, Z. H., Adams, M. W. W., and Rees, D. C. (1992) *Protein Sci. 1*, 1494−1507.
9. Britton, K. L., Baker, P. J., Borges, K. M. M., Engel, P. C., Pasquo, A., Rice, D. W., Robb, T., Scandurra, R., Stillman, T. J., and Yip, K. S. P. (1995) *Eur. J. Biochem. 229*, 688−695.
10. Yip, K. S. P., Baker, P. J., and Scandurra, R. (1995) *Acta Crystallogr., Sect. D 51*, 240−248.

11. DeDecker, B. S., O'Brien, R., Fleming, P. J., Geiger, J. H., Jackson, S. P., and Sigler, P. B. (1996) *J. Mol. Biol. 264*, 1072−1084.
12. Jaenicke, R., Schurig, H., Beaucamp, N., and Ostendorp, R. (1996) *Adv. Protein Chem. 48*, 181−269.
13. Russell, R. J. M., Ferguson, J. M. C., Hough, D. W., Danson, M. J., and Taylor, G. L. (1997) *Biochemistry 36*, 9983−9994.
14. Aguilar, C. F., Sanderson, I., Moracci, M., Ciaramella, M., Nucci, R., Rossi, M., and Pearl, L. H. (1997) *J. Mol. Biol. 271*, 789−802.
15. Auerbach, G., Huber, R., Grättinger, M., Zaiss, K., Schurig, H., Jaenicke, R., and Jacob, U. (1997) *Structure 5*, 1475−1483.
16. Fiala, G., and Stetter, K. O. (1986) *Arch. Microbiol. 145*, 56−60.
17. Brown, S. H., Costantino, H. R., and Kelly, R. M. (1990) *Appl. Environ. Microbiol. 56*, 1985−1991.
18. Kengen, S. W. M., Luesink, E. J., Stams, A. J. M., and Zehnder, A. J. B. (1993) *Eur. J. Biochem. 213*, 305−312.
19. Gueguen, Y., Voorhorst, W. G. B., van der Oost, J., and de Vos, W. M. (1997) *J. Biol. Chem. 272*, 31258−31264.
20. Laderman, K. A., Asada, K., Uemori, T., Mukai, H., Taguchi, Y., Kato, I., and Anfinsen, C. B. (1993) *J. Biol. Chem. 268*, 24402−24407.
21. Jorgensen, S., Constantin, V. E., and Antranikian, G. (1997) *J. Biol. Chem. 272*, 16335−16342.
22. Dong, G., Vielle, C., Savchenko, A., and Zeikus, J. G. (1997) *Appl. Environ. Microbiol. 63*, 3569−3576.
23. Dong, G., Vielle, C., and Zeikus, J. G. (1997) *Appl. Environ. Microbiol. 63*, 3577−3584.
24. Constantino, H. R., Brown, S. H., and Kelly, R. M. (1990) *J. Bacteriol. 172*, 3654−3660.
25. Voorhorst, W. G. B., Eggen, R. I. L., Luesink, E. J., and de Vos, W. M. (1995) *J. Bacteriol. 177*, 7105−7111.
26. Bauer, M. W., Bylina, E., Swanson, R., and Kelly, R. M. (1996) *J. Biol. Chem. 271*, 23749−23755.
27. Kempton, J. B., and Withers, S. G. (1992) *Biochemistry 31*, 9961−9969.
28. Withers, S. G., Rupitz, K., Trimbur, D., and Warren, R. A. J. (1992) *Biochemistry 31*, 9979−9985.
29. Street, I. P., Kempton, J. B., and Withers, S. G. (1992) *Biochemistry 31*, 9970−9978.
30. Namchuk, M. N., and Withers, S. G. (1995) *Biochemistry 34*, 16194−16202.
31. Wang, Q., Trimbur, D., Graham, R., Warren, R. A. J., and Withers, S. G. (1995) *Biochemistry 34*, 14554−14562.
32. Conchie, J., and Levvy, G. A. (1963) *Methods Carbohydr. Chem. 45*, 273.
33. Ballardie, F., Capon, B., Sutherland, J. D. G., Cocker, D., and Sinnott, M. L. (1973) *J. Chem. Soc., Perkin Trans. 1*, 2418.
34. Sinnott, M. L., and Souchard, I. J. L. (1973) *Biochem. J. 133*, 81.
35. Nath, R. L., and Rydon, H. N. (1954) *Biochem. J. 57*, 1.
36. Adams, M. W. W. (1995) *Archaea: A Laboratory Manual*, pp 3.47−3.49, Cold Springs Harbor Laboratory Press, Cold Springs Harbor, NY.
37. Bryant, F. O., and Adams, M. W. W. (1989) *J. Biol. Chem. 264*, 5070−5079.
38. Bradford, M. M. (1976) *Anal. Biochem. 72*, 248−254.
39. Wilkinson, G. N. (1961) *Biochem. J. 80*, 324.
40. Makhatadze, G. I., Medvedkin, V. N., and Privalov, P. L. (1990) *Biopolymers 30*, 1001−1110.
41. Freire, E., and Biltonen, R. L. (1978) *Biopolymers 17*, 463−479.
42. Sambrook, J., Fritsch, E. F., and Maniatis, T. (1989) in *Molecular Cloning: A Laboratory Manual*, 2nd ed., pp 18.64−18.68, Cold Spring Harbor Laboratory Press, Cold Spring Harbor, NY.
43. Bidlingmeyer, B. A., Cohen, S. A., and Tarvin, T. L. (1984) *J. Chromatogr. 336*, 93−104.
44. Edelhoch, H. (1967) *Biochemistry 6*, 1948−1954.
45. Riddles, P. W., Blakely, R. L., and Zerner, B. (1983) *Methods Enzymol. 91*, 49−60.
46. Day, A. G., and Withers, S. G. (1986) *Biochem. Cell Biol. 64*, 914−922.
47. Barlin, G. B., and Perrin, D. D. (1966) *Q. Rev. Chem. Soc. 20*, 75.
48. Kortum, G., Vogel, W., and Andrussow, K. (1961) *Pure Appl. Chem. 1*, 450.
49. Robinson, R. A., Davis, M. M., Paabo, M., and Bower, V. E. (1960) *J. Res. Natl. Bur. Stand., Sect. A 64*, 347.
50. Ba-Saif, S. A., and Williams, A. (1988) *J. Org. Chem. 53*, 2204.
51. Withers, S. G., and Rupitz, K. A. (1990) *Biochemistry 29*, 6405−6409.
52. Gabelsberger, J., Liebl, W., and Schleifer, K.-H. (1993) *FEMS Microbiol. Lett. 109*, 131−138.
53. Grogan, D. W. (1991) *Appl. Environ. Microbiol. 57*, 1644−1649.
54. Moracci, M., Nucci, R., Febbraio, F., Vaccaro, C., Vespa, N., La Cara, F., and Rossi, M. (1995) *Enzyme Microb. Technol. 17*, 992−997.
55. Fersht, A. R. (1988) *Biochemistry 27*, 1577−1580.
56. Sinnott, M. L. (1990) *Chem. Rev. 90*, 1171.
57. Legler, G. (1990) *Adv. Carbohydr. Chem. Biochem. 48*, 318−384.
58. Biggs, A. I., and Robinson, R. A. (1961) *J. Chem. Soc.*, 388−393.
59. Jencks, W. P. (1972) *Cold Spring Harbor Symp. Quant. Biol. 36*, 1−11.
60. Kajimoto, T., Liu, K., Pederson, R. L., Zhong, Z., Ichikawa, Y., Porco, J., and Wong, C.-H. (1991) *J. Am. Chem. Soc. 113*, 6187−6196.
61. Hennig, M., Darimont, B., Sterner, R., Kirschner, K., and Jansonius, J. N. (1995) *Structure 3*, 1295−1306.
62. Barrett, T., Suresh, C. G., Tolley, S. P., Dodson, E. J., and Hughes, M. A. (1995) *Structure 3*, 951−961.

BI9814944